applied sciences

MDPI

Article

Loads on the Knee Joint Ligaments during Stair Climbing

Carlo Albino Frigo, Maddalena Grossi and Lucia Donno *

Movement Biomechanics and Motor Control Lab, Department of Electronics, Information and Bioengineering, Politecnico di Milano, I-20133 Milan, Italy; carlo.frigo@polimi.it (C.A.F.); maddalena.grossi@mail.polimi.it (M.G.)
* Correspondence: lucia.donno@polimi.it

Featured Application: Climbing stairs is both a common and highly demanding motor task. Knowledge of ligament loads during this movement could be useful for planning reconstruction surgery, for providing suggestions to subjects with ligament injuries, and for identifying possible compensatory strategies for the reduction of these loads.

Abstract: Background. Stair climbing is often performed by people in daily life and requires considerable energy and muscle effort. This task has been widely described in the literature, but the role of the knee joint ligaments has not been sufficiently investigated. This could be relevant for planning ligament reconstruction surgery, for providing suggestions to subjects with partial ligament injuries, and for identifying compensatory strategies for reducing ligament loads. Methods. A dynamic musculoskeletal model was used to analyse the relationship between ligament loads and muscle forces during stair climbing. Results. The most loaded ligaments were the posterior cruciate ligament and the deep fibres of the medial collateral ligament, particularly during the mid-swing phase, where the knee was maximally flexed and the hamstring muscles contracted. The anterior cruciate ligament was recruited during the stance phase to compensate for the anteriorly-directed force applied to the tibia by the vasti muscles; the collateral ligaments stabilized the knee joint during the swing phase. The tibiofemoral contact force, resulting from all external and internal forces applied to the knee, was in good agreement with data provided in the literature. Conclusions. This study represents a forward step in the knowledge of ligament loads during stair climbing, which could be useful for providing informed recommendations to subjects with ligament injuries.

Keywords: stair climbing; knee joint ligaments; musculoskeletal model; dynamic simulation; knee joint biomechanics

Citation: Frigo, C.A.; Grossi, M.; Donno, L. Loads on the Knee Joint Ligaments during Stair Climbing. *Appl. Sci.* **2023**, *13*, 7388. https://doi.org/10.3390/app13137388

Academic Editors: Andrzej Wit and Roozbeh Naemi

Received: 30 May 2023
Revised: 14 June 2023
Accepted: 20 June 2023
Published: 21 June 2023

1. Introduction

Climbing stairs is a common task that people perform quite frequently in normal daily life. It is also a recommended exercise for people who want to maintain good physical shape without getting involved in more demanding training [1–4]. Many biomechanical studies have shown that stair climbing entails considerable effort in terms of energy consumption and muscle activity [5–8], and that it is more physically and mechanically challenging than level walking [9] because greater net joint moments are required of the lower limb muscles. Stair climbing is such a crucial task in daily life that many studies concerning knee joint arthroplasty (total or unicompartmental reconstruction) aim at restoring the native knee kinematics and stability during this movement [10–13]. The joints are loaded with relevant moments and forces, and the neural control system is involved in maintaining balance and in dealing with the geometry of the steps [14–16]. It is therefore understandable that elderly people [17] or people with control-system deficits, cardiovascular problems, muscle weakness, joint pains, and osteoarthritis [18,19] have difficulty climbing stairs and therefore have a worsened quality of life. As for the knee joint, which is the most loaded joint, the large range of movement associated with strong muscle contractions places the internal structures, cartilage, and ligaments, in a very demanding situation

and can even lead to risk of damage. Several studies have analysed the loads at the tibiofemoral interface and at the patellofemoral joint [20–26], but, as far as we are aware, none of them has described the role of the ligaments in stair climbing and the forces they support to keep the joint congruent. Actually, some attempts to measure ligament strain in vivo have been made [27,28] by means of a strain-gauge device (DVRT). In particular, Fleming et al. [29] measured the strain of the Anterior Cruciate Ligament in vivo during stair climbing. This method only measures the deformation of a few ligaments, and, from these measurements, it is difficult to obtain the load distribution among several ligaments. In this sense, musculoskeletal models represent an innovative method for studying the biomechanics of complex structures, having the potential to simulate the movement, to apply the muscular forces, and to estimate the loads in all internal structures of a joint. Since knowledge of ligament loads can be useful for providing suggestions to subjects with partial injuries of the ligaments and for identifying any compensatory strategies for the reduction of these loads, we have deemed it important to deepen understanding of the relationship between ligament loads and muscle forces. For this purpose, we have adapted a previously developed musculoskeletal model [30] to the analysis of stair climbing. This work is based on a single, exemplary subject, and does not pretend to represent any specific population. The aims of this study were to assess how the different knee-joint ligaments are loaded in an intact knee during stair climbing and to explain how ligament tensions are affected by the muscle forces produced in this specific task. Deeper investigation will be devoted to analysing how the muscle forces should be modulated to reduce the risk of ligament damage.

2. Materials and Methods

2.1. The Model

Our biomechanical model is composed of two parts. The first is made of geometric solids representing the trunk, the pelvis, the thighs, the shanks, and the feet, joined with each other by revolute joints. These joints can be animated using angular coordinates obtained from the movement analysis of an experimental subject. For this reason, it will be named 'the driving' model. The second structure is a musculoskeletal model of the lower limb, which includes the femur, the tibia and fibula, the rotula, the foot as a rigid body, the knee ligaments, and the muscles. This model reproduces the tibiofemoral and the patellofemoral interactions by imposing a no-penetration constraint between the bone contact surfaces. The main ligaments, represented by spring elements with nonlinear characteristics, serve to maintain the bones' attachment to each other while permitting their relative movements. To measure the relative rotation and translation of the tibia in relation to the femur, an articulated mechanism (that we called 'the Grood and Suntay—G&S mechanism') was attached to the bones. As shown in Figure 1, it was composed of three mutually orthogonal revolute joints, representing flexion/extension (Flex/Ext), adduction/abduction (Add/Abd), and internal/external rotation (Int/Ext rot).

The first joint (red in the Figure 1) connects Shaft 1 to Plate 1; the second (green) connects Plate 1 to Plate 2; the third (blue) connects Plate 2 to Shaft 2. The latter was connected to Shaft 3 by a special constraint that imposes parallelism of the two shafts (same orientation) without any limitation to the relative displacements. Shaft 1 was then rigidly connected to the femur with the flexion/extension axis aligned with the medial and lateral epicondyles. Shaft 3 was rigidly connected to the tibia, oriented as its longitudinal axis. Any relative movement between the tibia and the femur could then be measured using the rotation angles of the three revolute joints, and by the relative coordinates x, y, z provided by the parallelism constraint. This measurement convention is the same one proposed by Grood and Suntay [31], and this is the reason for the name we assigned to this mechanism.

To connect the two parts of our model, the femur was rigidly attached to the solid representing the thigh in such a way that the flexion/extension axis (red) of the G&S mechanism coincides with the flexion/extension axis attached to the thigh. Then the flexion/extension movement was transmitted to the tibia by converting the flexion/extension revolute joint

of the G&S mechanism into a motor having the same rotation axis. In this way, just the flexion/extension degree of freedom is constrained, while the remaining adduction/abduction, internal/external rotation, distal-proximal, medio-lateral, and anterior-posterior displacements are free. They can be measured as outputs of the revolute joints and of the parallelism constraint. As a result of this arrangement, the relative movement between the tibia and femur during flexion/extension is determined by: (a) the geometry of the articulating surfaces; (b) the ligament tensions; (c) the external forces (ground reactions and inertia forces); and (d) the muscle forces.

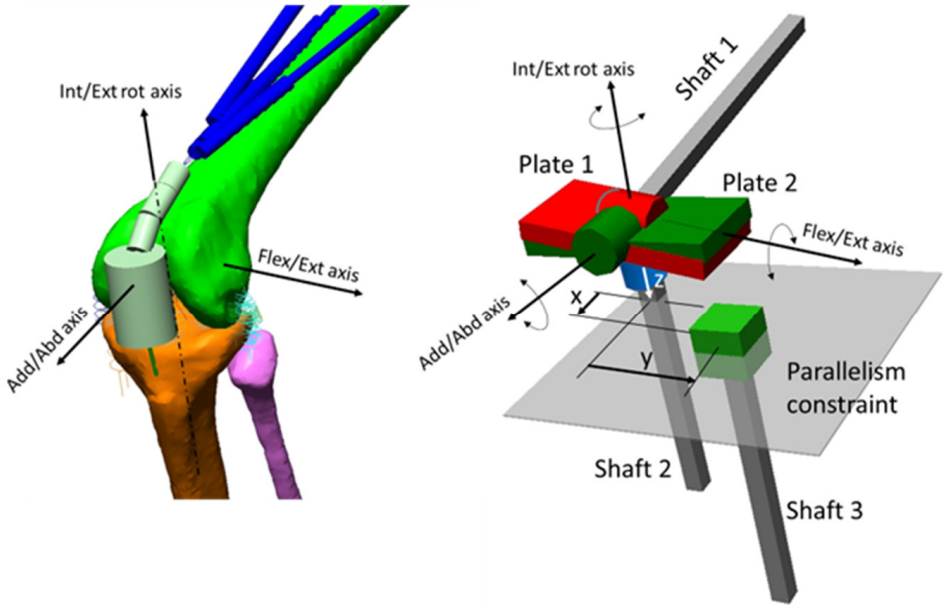

Figure 1. On the right, the so-called G&S mechanism used to measure the six d.o.f and to impose the flexion/extension movement. On the left, the G&S mechanism included in the knee joint model with the corresponding functional axes.

The ground reaction force, which is applied to a time-varying specific point on the foot, is transferred to the tibia in a point corresponding to the centre of the knee and the transfer moment is applied to the tibia. This loading condition is equivalent to the original one but is not affected by abnormal deviations in the trajectory of the foot, which could occur because of irregularities in the contact surfaces of the knee. All the main muscles acting at the knee are represented by linear actuators that can develop a force corresponding to a predefined muscle contraction.

The details of the whole biomechanical model can be found in previous publications [25,30,32,33]. Here we report the main features of the model:

2.1.1. The Driving Model

This is the model part composed of geometric solids. The trunk and the pelvis are represented by two boxes, the thighs and shanks by cylinders, and the feet by extrusion solids; the pelvis is connected to the trunk by three mutually orthogonal revolute joints that allow control of pelvis anteversion, lateral tilt, and horizontal rotation respectively. The hip joints are reproduced by three mutually orthogonal revolute joints allowing flexion/extension, adduction/abduction, internal/external rotation; the knees have two revolute joints allowing the flexion/extension and internal/external rotation; the ankle joint allows plantarflexion/dorsiflexion and pronation/supination of the foot.

2.1.2. The Musculoskeletal Model

The bone components were obtained from magnetic resonance images (MRI) taken of a normal subject, male, 172 cm tall, weighing 70 kg. The following ligaments were

considered: the anterior (ACL) and the posterior (PCL) cruciate ligaments, each of them composed of an anterior and a posterior bundle; the medial (MCL) and the lateral (LCL) collateral ligaments, each of them composed of an anterior, an intermediate and a posterior bundle; the deep component of the MCL, subdivided in anterior and posterior bundles; the antero-lateral and posterior capsula, composed of a lateral and a medial bundle. Each ligament was characterised by a force-length relationship that included a quadratic rise of the force up to a predefined strain limit, and a linear behaviour for larger deformations. This relationship is described by the following equations [34]:

$$f = \begin{cases} 0.25K\,\varepsilon^2/\varepsilon_l, & 0 \le \varepsilon \le 2\varepsilon_l \\ K(\varepsilon - \varepsilon_l), & \varepsilon > 2\varepsilon_l \\ 0, & \varepsilon < 0 \end{cases} \quad (1)$$

in which K is the stiffness (N/m) in the linear interval of the curve, ε is the strain of the ligament, and ε_l represents the strain limit corresponding to the intercept of the linear section with the abscissa. All parameters concerning the attachment points and the force-length relationship were obtained from the literature and adapted to our model as described in the previous publication [30]. The rotula was approximated to a cylinder that could slide inside the femoral trochlea. The patellar tendon was considered an inextensible rod. The following muscles were included in the model: rectus femoris (RF); lateral, intermedial and medial vasti (VL, VI, and VM respectively); hamstrings (semitendinosus—ST, semimembranosus—SM, biceps femoris long head—BFlh, biceps femoris short head—BFsh); lateral and medial gastrocnemius (GAl and GAm respectively); gluteus minimum (GLmin); gluteus maximum (GLmax); gluteus medius (GLmed); iliacus (IL); psoas (PS); tensor fascia latae (TFL); tibialis anterior (TA); peroneus (PE); and soleus (SO).

2.2. The Inputs to the Model

From a previous data collection [6], we extracted the kinematics and ground-reaction forces referring to a subject of body mass and height similar to the one referred to by the MRI. The subject was climbing a staircase equipped with load cells in three of its steps. The steps were 17 cm high and 29 cm deep. The data collected in the cited study were used as a normality band, which refers to ten healthy male subjects (1.79 $\pm$ 0.05 m of body height, 82.2 $\pm$ 8.5 kg of body mass and 28.8 $\pm$ 2.9 years).

The acquisition time (approximately 2.8 s) included a full stride cycle of the left foot, from initial contact (IC) on a sensored step to the next IC two steps higher. Initial contact occurred at time 0.7 s from the acquisition start, and the stride cycle lasted about 1.4 s. The right IC occurred 0.7 s after the left IC.

A three-dimensional representation of the staircase was generated and imported into the same software used for the implementation of the biomechanical musculoskeletal model (SimWise-4D, Design Simulation Technologies, DST, Canton, MI, USA), as show in Figure 2. When the model was related to the staircase, there were some discrepancies between the position of the feet and the surface of the steps. This was predictable, in that the size of the model was not exactly the size of the subject the kinematic data belonged to. Thus, we slightly changed the bone lengths in the model in order to have the right and the left feet reaching their relative steps with minimum clearance and no collision with the border. Then we applied the ground reaction force to the proximal tibia in correspondence with the centre of the knee joint and the moment to compensate for this transfer, as previously described. This transfer moment was computed by running the computation program with segment masses set at zero. In this way, the contribution of the inertia components was nil, and the knee-joint moment was the result of the ground reaction force only. To compute the muscle forces, the lever arms of each muscle in relation to the joint rotation axes are required. Due to the complexity of the knee joint, which in our model does not have a fixed rotation axis, and to the multiple functions of several muscles, the lever arms cannot be computed analytically. So we ran several simulations of stair climbing in which

the masses were set at zero, as were ground reaction forces and moments, and only one muscle at a time was activated with a constant predefined force of 100 N. We measured the moments at each rotation axis and divided those values by 100 N. The result was the desired lever arm. We also needed to know the joint moments around each rotational axis. These moments were obtained via the motion-analysis software available on the system (BTS Bioengineering SpA, Garbagnate Milanese (MI), Italy). Then we implemented an algorithm to compute the muscle forces with the objective that the maximum specific force (that is, force divided by physiologic cross-sectional area—PCSA) was minimal (Min/Max algorithm) [35]. The PCSA of the muscles involved were obtained from the literature [5]. The constraints were: (a) the sum of the moments produced by each muscle at each rotation axis had to be equal to the moment computed around that axis; (b) all muscle forces had to be greater than or equal to zero.

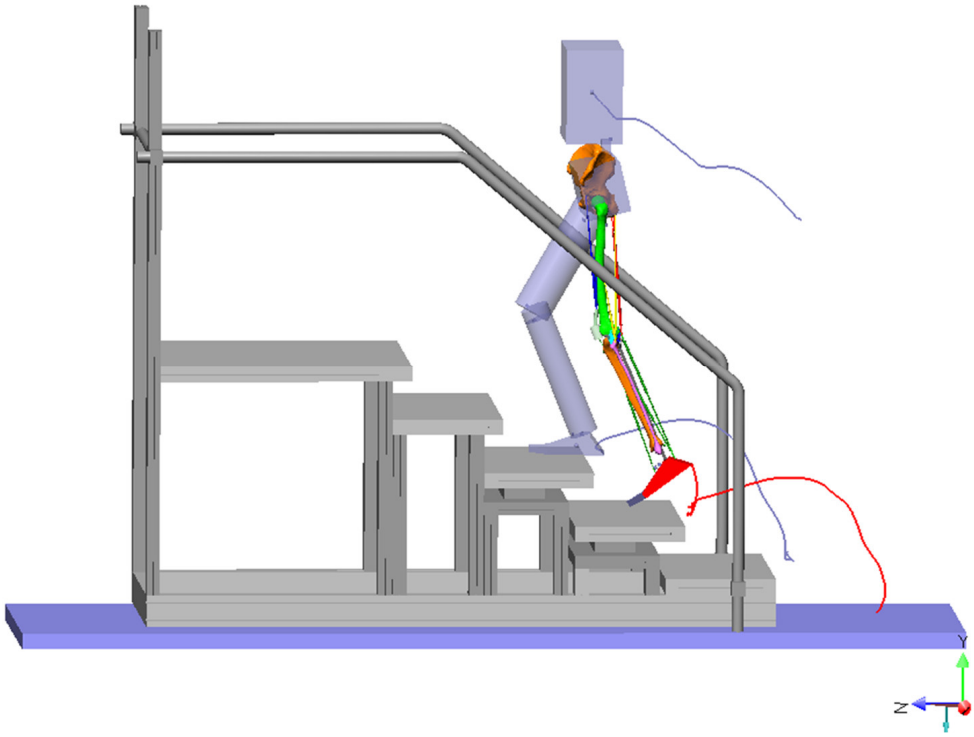

Figure 2. The driving model. The trajectory of the centre of the trunk and of right and left feet (the heels) are represented.

The results of our simulations were smoothed by a moving average filter.

3. Results

In Figure 3, the kinematic inputs to the model are depicted. The forward displacement of the trunk progressed almost linearly with time (400 mm/s); the medio-lateral displacement was oscillating with an amplitude of 100 mm, having the minimum and maximum in correspondence with the initial contacts of ipsilateral and contralateral foot respectively (50% of the stride cycle); the trunk translated by 170 mm in the vertical direction at each step, consistently with the step height.

As to the joint angles, our data belong to the normal band (average ± SD) reported in a previous publication [6]. The normal band reported a maximum flexion angle of the hip equal to 71° on average ±9.5° SD, while our exemplary subject achieved a maximum flexion angle of 66°, a maximum flexion angle of the knee of 93° ± 8.1° SD (87° in our subject), and a maximum ankle plantarflexion angle of 22° ± 7.7° SD (23° in our subject).

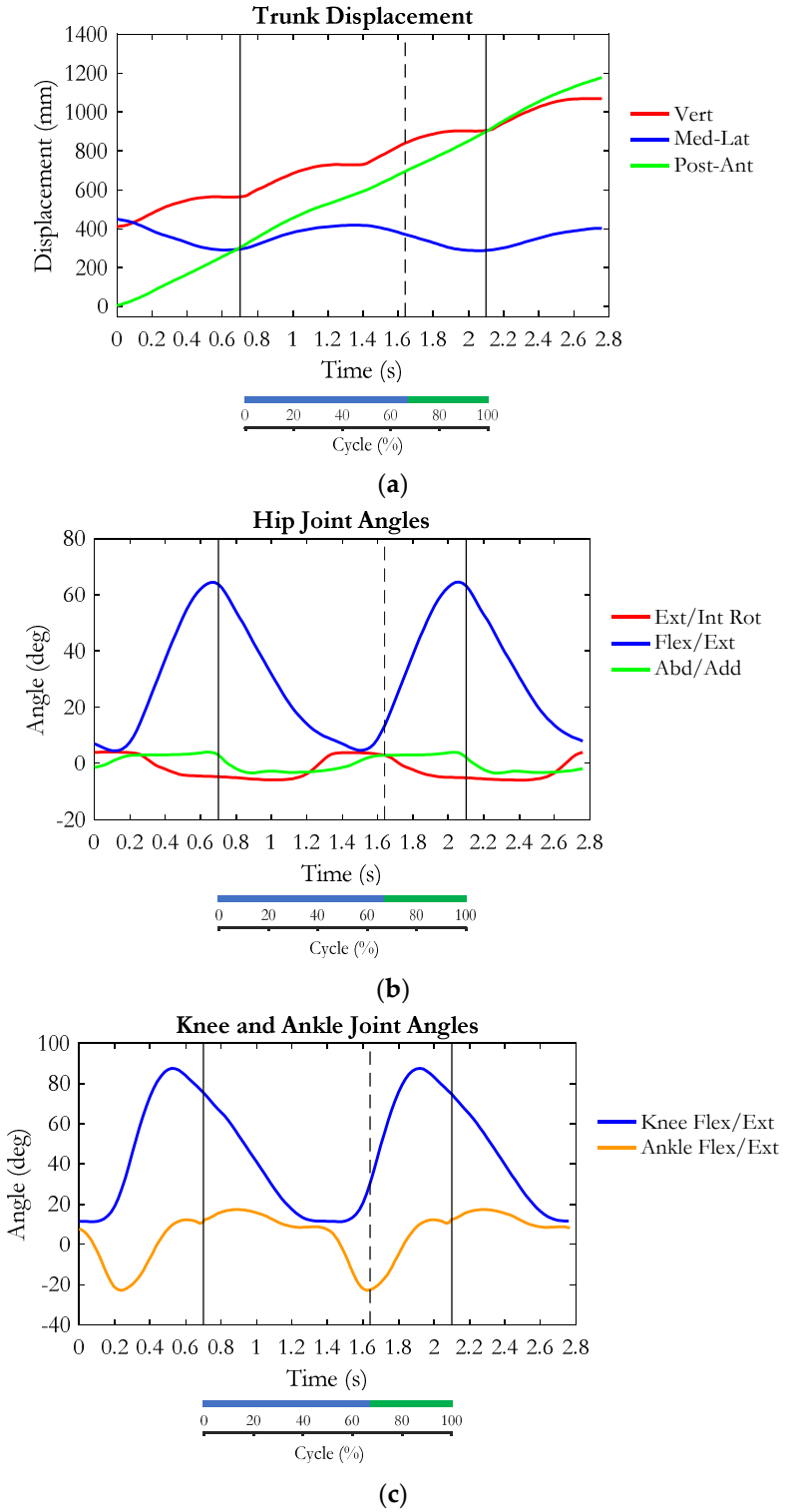

Figure 3. Kinematic input to the model. The 3D coordinates of the centre of the trunk segment: (**a**) medial-lateral (Med–Lat), vertical (Vert), posterior-anterior (Post–Ant); (**b**) 3D angles of the Hip (flexion/extension, adduction/abduction, internal/external rotation); (**c**) Knee and Ankle joint flexion/extension angles. Continuous vertical lines represent the two ICs, while the dashed line refers to the toe off event. Blue and green intervals in the horizontal bar mark the stance and the swing phase, respectively.

During the dynamic simulation of stair climbing, the maximum hip-joint flexion (about 66°) was reached in correspondence with the initial contact, while the maximum

knee flexion (87°) occurred in the late swing phase, before IC. At initial contact, the knee was flexed by 77° and the ankle had a dorsiflexion angle of 11°. Then, during hip and knee extension, the ankle underwent a slight dorsiflexion and then returned to the initial contact angle when the knee was maximally extended. Ankle plantarflexion started about 250 ms before toe off and reached the maximum plantarflexion angle (23°) at the time of toe off. During the stance phase, the hip joint exhibited a slight abduction, while in the swing phase it was slightly adducted. On the transversal plane, except for the terminal stance phase, the hip joint preserved its external rotation.

Figure 4 represents the GRF applied to the upper extremity of the tibia (left) and the corresponding transfer moment (right).

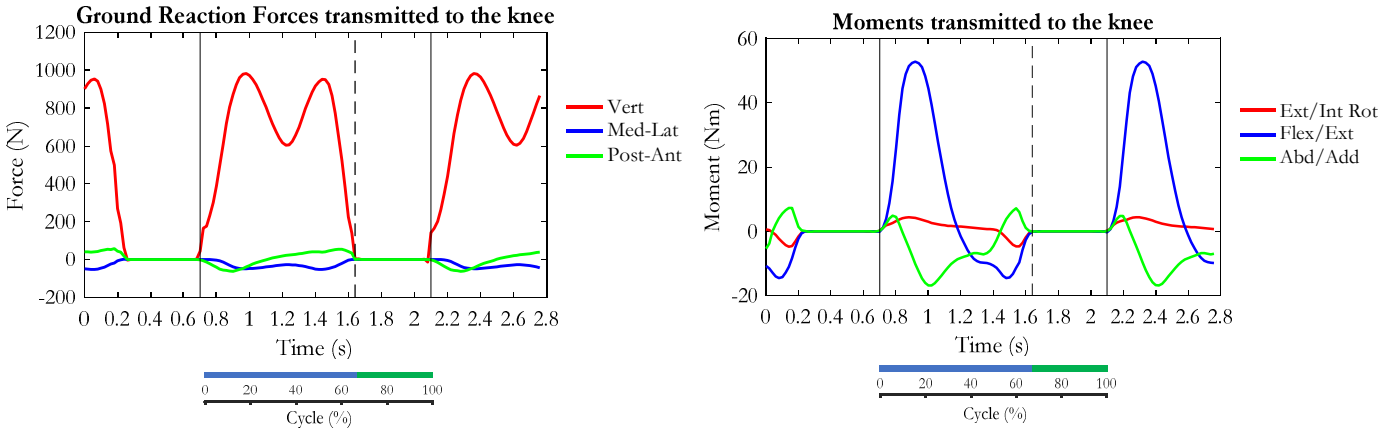

(**a**) (**b**)

Figure 4. Dynamic input to the model: (**a**) ground reaction forces (GRF)—mediolateral, vertical, posteroanterior—; (**b**) moments applied to the tibia to compensate for the transfer of the GRF to the centre of the knee joint: flexion/extension, external/internal rotation, adduction/abduction.

The stance phase of stair climbing was characterised by the double bump of the vertical force component, with, in this case, the first peak (980 N) slightly higher than the second one (953 N). At one third of the stance phase, the GRF anterior-posterior component changed from posterior to anterior. The medio-lateral component was directed medially for the whole stance phase. As depicted in Figure 4, the transfer moment was nil during the swing phase because of the non-contact between the foot and ground (GRF was zero). During the stance phase, the moment transferred at the knee joint was flexor in the first half of the stance phase and extensor in the second. On the frontal plane, the knee joint experienced an adduction moment during most of the stance phase, except for the final interval. An external rotation moment was applied to the knee for most of the stance phase, followed by an internal rotation moment at the end of the stance phase.

In Figure 5, the estimated muscle forces referring to the muscles of interest for the knee joint are reported.

Among the extensor muscles (Figure 5a), the VL and the VM proved to be the most involved ones, expressing the highest force (887 N). They were activated after the initial contact, concurrently with the knee extension. Then, a smaller peak of force appeared during the terminal stance phase. During the swing phase, during the large knee flexion, the vasti muscles were inactivated, while a small activation of the RF was observed in conjunction with the hip flexion in preparation to the second IC.

Among the hamstring muscles (Figure 5b), which are extensors for the hip and flexors for the knee, the SM expressed its maximum force (300 N) in the load acceptance phase (early stance phase). Then, a second peak of force of approximately 114 N appeared during the terminal stance phase, in conjunction with the knee flexion. During the swing phase, in which the large knee flexion occurred, the BFsh produced an almost constant force of 80 N. The GAl and GAm (Figure 5c) exhibited an increasing contraction force throughout most

of the stance phase and achieved a maximum at the terminal stance phase (push-off), at the beginning of ankle plantarflexion.

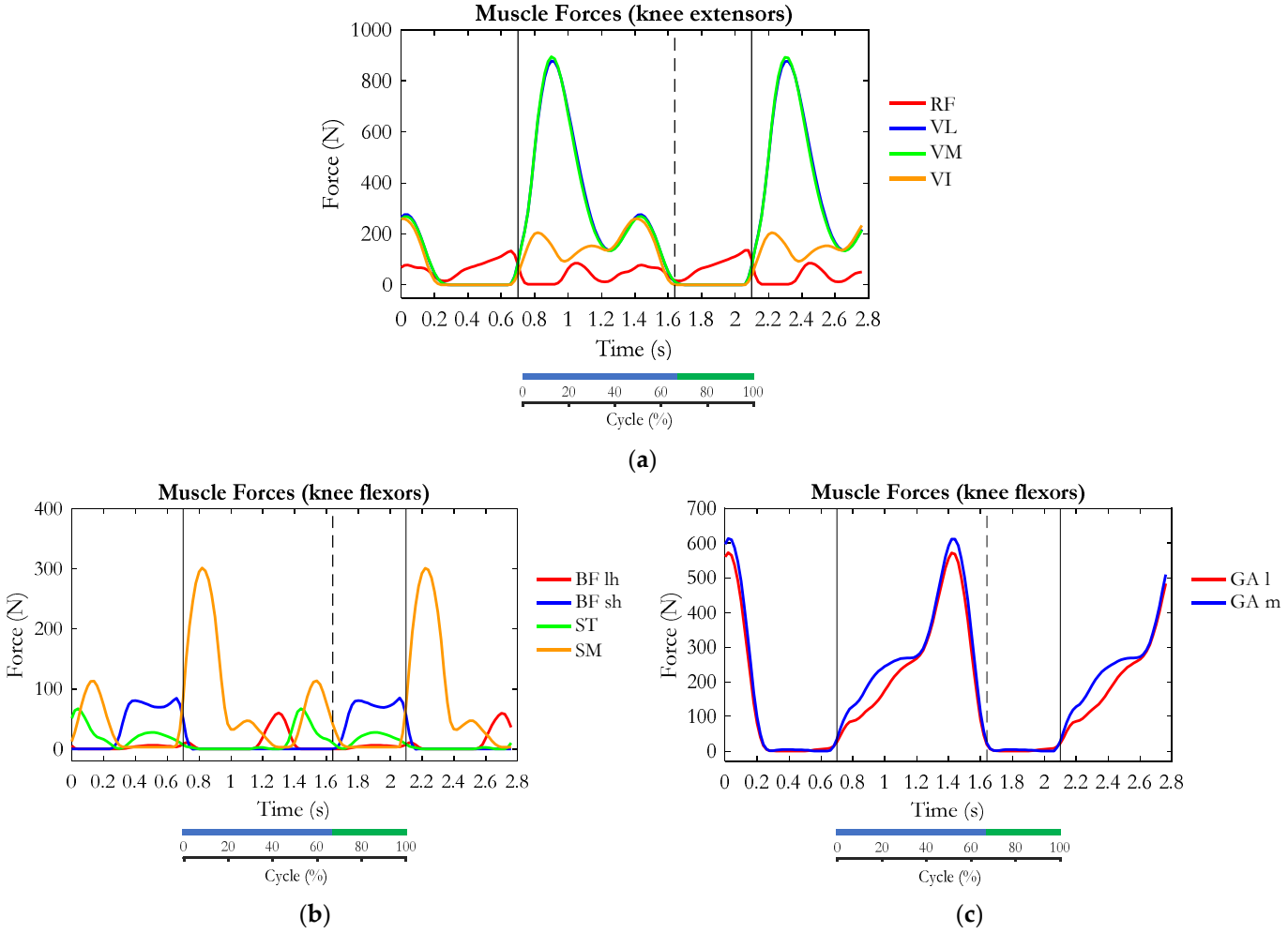

Figure 5. Dynamic input to the model: muscle forces. Among all muscles considered in the procedure for muscle forces estimation, only the muscles acting at the knee joint are reported here: (**a**) the quadriceps components; (**b**) the hamstring group; and (**c**) the two gastrocnemii.

The pattern of the contact force between the femoral condyles and the tibial plateaux during climbing stairs is depicted in Figure 6. The distal-proximal component showed a double bump during the stance phase, with the first peak (2624 N) smaller than the second one (3225 N). In correspondence with toe off, the contact force was at its lowest value, equal to 166 N. Then it rose and reached a plateau of approximately 755 N in the mid-swing phase. As to the medio-lateral and anterior-posterior components, they both reached their maximum values (approximately 280 N and 930 N, respectively) slightly before the mid stance phase.

The forces supported by the cruciate and collateral ligaments are depicted in Figure 7. The maximum tension was developed by the PCL, with two peaks, one at the initial stance phase (approximately 300 N), and the second, slightly smaller, at the mid swing phase. This ligament was relaxed during mid stance and its tension slightly rose to a minor peak (50 N) just before toe-off. At the difference, the ACL was tensioned at the mid and late stance phases, just after the PCL relaxation, when it reached a peak of approximately 134 N. It was completely relaxed at toe-off and during the swing phase.

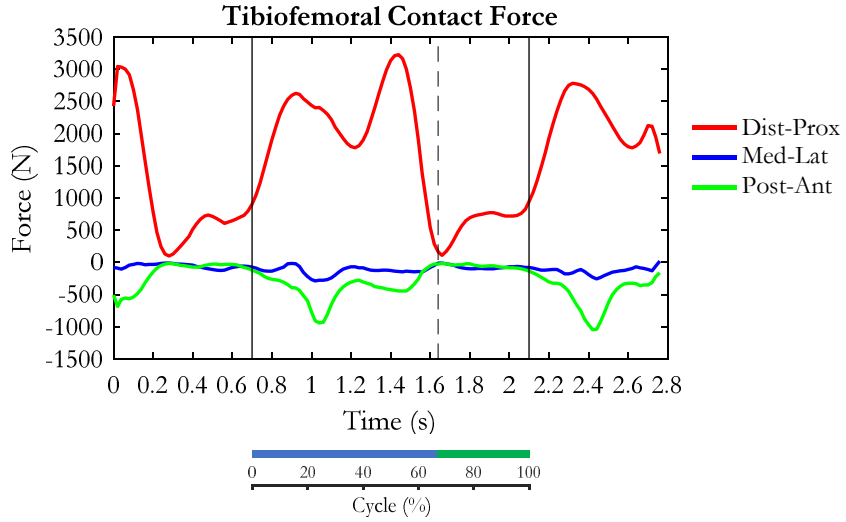

Figure 6. Output of the model: the tibiofemoral contact forces: medial-lateral (Med–Lat), distal-proximal (Dist–Prox), posterior-anterior (Post–Ant).

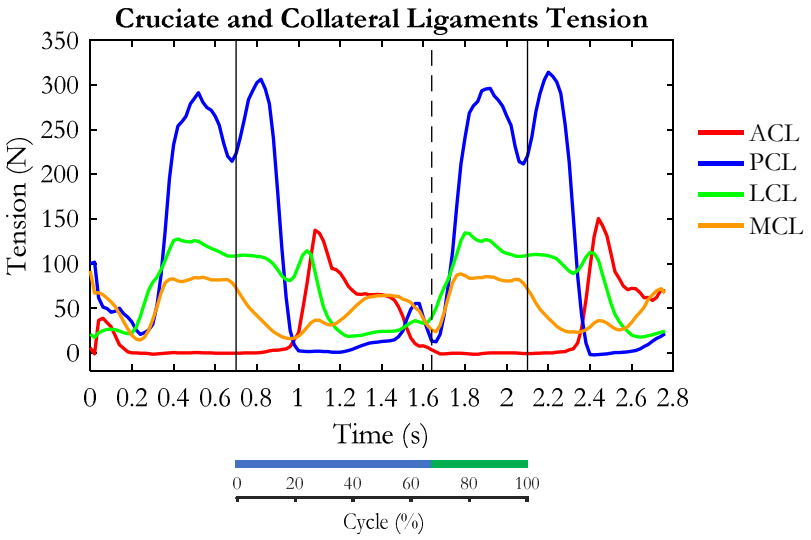

Figure 7. Output of the model: the ligament tensions. The anterior cruciate, posterior cruciate, lateral collateral, and medial collateral forces include the contributions of their different bundles.

The MCL was recruited during the swing phase and experienced a relief at the initial stance phase. Then it was recruited during mid and late stance phases. The LCL recruitment occurred during mid and late swing phases and lasted until the mid-point of the stance phase. During the swing phase, the recruitment of the two collateral ligaments appeared to be synergistic, with LCL expressing a maximum tension larger than MCL (164 N vs. 87 N).

The tension of the deep components of MCL (MCL-deep) and the capsular ligaments are reported in Figure 8. Similarly to the superficial bundles of MCL, MCL-deep was gradually relieved after the initial contact and recruited during the mid-terminal stance phase and swing phase, in which it expressed its maximum tension of 253 N.

The fibrous capsule appeared relieved during the swing phase. Specifically, the lateral bundles of the anterior (Cap-Ant-Lat) and posterior (Cap-Post-Lat) fibrous capsule were recruited at the early stance phase, while the posterior-medial structure (Cap-Post-Med) was loaded during the mid stance phase.

Among all ligament structures, the PCL and the MCL-deep exhibited the highest tension (approximately 300 N and 250 N, respectively).

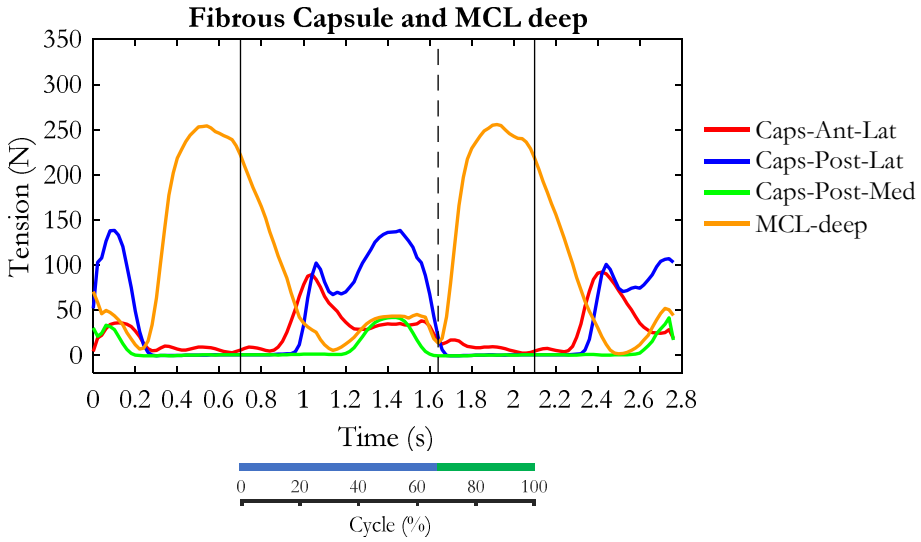

Figure 8. Output of the model: tension of the different capsule components and deep MCL.

4. Discussion

The present study was designed to investigate the loads on internal knee joint structures during the relatively demanding task that is stair climbing. In particular, we were interested to know how the ligament tensions were related to the joint kinematics and muscle forces. This problem is of clinical interest because of its implication in rehabilitation and surgery planning, such as knee-joint arthroplasty and ligament reconstruction. A dynamic musculoskeletal model was adopted for this purpose, and was animated using data extracted from our repository [6]. This was just an exemplary analysis, referring to the specific anthropometry and pattern of movement of a single subject. Deeper investigation will be devoted to analysing the effects of subject size in relation to the step geometry (riser and tread) and the effects of gender and age. Developing a subject-specific model to be used in clinical practice could be an additional goal, with the aim of predicting the effects of ligament reconstruction or ligament removal in case of knee-joint arthroplasty.

In our single case study, the pattern of muscle forces and tibiofemoral contact forces were obtained by taking into account ground-reaction forces, inertia forces and moments, the lever arms of muscles in relation to each joint rotational axis, and implementing an optimisation algorithm that minimises the maximum specific force. The phasic activities of the muscles acting on the knee joint predicted by the algorithm were in agreement with the data obtained in [36] through electromyography measurements on ten healthy young male subjects during stair climbing. As to the muscle forces, the contributions of different muscles to stair climbing is in good agreement with their function: the whole quadriceps was mostly active during the stance phase (see Figure 5a), with the VM and the VL exhibiting a high peak of contraction force (900 N) in the first half of the stance phase, thus confirming their main roles as knee extensors. The second peak of their activity corresponds to the peak of the gastrocnemius force (Figure 5c). This can be explained by considering the double-joint arrangement of the gastrocnemii (GAl and GAm). They are biarticular muscles acting as ankle plantar flexors and knee flexors. At late stance, they contribute to pushing off by producing a plantarflexion moment at the ankle joint. This entails a flexor effect at the knee, and thus the need for extensor muscles to counteract this effect. Differently from the rest of the quadriceps, the RF is active during the swing phase also, thus contributing to the hip-flexor moment required to raise the thigh and foot above the next step. Among the hamstring muscles (Figure 5b), the most intense force is produced by the SM at the beginning of stance phase. This is apparently in contradiction with the need for an extensor moment at that time. The problem of co-contraction of the quadriceps and hamstrings, when apparently only knee extension is required, has been deeply investigated in reference to the cycling task [37,38] where a similar condition

occurs. The phenomenon is called 'Lombards' paradox' [39] and has been explained by considering the need to produce an extensor moment at the hip joint simultaneously with knee extension. In order to allow the SM to produce an extensor moment at the hip, the flexor moment produced at the knee must be counteracted by an additional activity of the extensor muscles. The effectiveness of this co-contraction of knee antagonist muscles depends on the ratio between the lever arms of the hamstring at the hip and knee [40]. Probably for this reason, the BFlh and the ST have different actions than the SM. Their main activity appears at mid and late stance, where knee flexion initiates. At late stance, the SM exhibits a peak of force as well. The hamstring activity during this phase is used to produce the extensor moment at the hip which, according to a previous publication [6], is required in this phase.

The tibiofemoral force, which is the result of all internal and external forces applied to the knee, showed a distal-proximal component with two peaks during the stance phase (the second higher than the first one), a minimum at toe off, and a slow rise to a plateau during the swing phase, which could be mainly due to the activity of BFsh, ST, and RF. This pattern was in perfect agreement with those obtained through the direct measurement of forces in sensorised prostheses during walking up stairs [22,26]. The difference in the force amplitude (about three times body weight in the reported publications, about four times body weight in our study) would probably depend on the different subjects considered: operation by knee arthroplasty, in case of the direct measurement, and one representative subject of a healthy population in our case. This makes us confident that our predictions of muscle force and ligament tension were reasonably accurate.

To our knowledge, this is the first study trying to quantify the load supported by the knee ligaments during stair climbing. A unique study in the literature dealing with the ligament loads during this task was conducted in vivo by Fleming et al. [29] and it focused only on the ACL. The cited authors reported that the ACL reached the maximum strain in correspondence with a knee-flexion angle of about 20°, which is in accordance with our results (see Figures 3c and 7).

As to role of the ligaments, our data show that the PCL supports the highest loads (about 300 N) followed by the deep fibres of the MCL (about 250 N). Both ligaments have a peak at mid swing, where the knee was maximally flexed (almost 90°) and the ST and the BFsh were contracted to brake the forward movement of the shank. Actually, during the swing phase, the RF was also activated, but probably because of the high flexion degree it had no relevant effect in the direction tangential to the tibial plateaux. Hence, a net posteriorly-directed force was applied to the proximal tibia, loading the PCL. Moreover, during the swing phase the gastrocnemii (antagonist of ACL) were relaxed. In fact, in this phase the tibialis anterior was activated for producing the ankle dorsiflexion (visible in Figure 3c) needed to avoid contact between the foot and the steps. The PCL force showed another peak occurring just after initial contact, where the knee was still flexed and was extending because of quadriceps contraction, but having a peak of the SM force at the same time. It is evident that the backwards-directed SM force is responsible for the backwards displacement of the tibia, and consequently for PCL loading in this phase. In fact, the force applied by the patellar tendon was likely to be perpendicular to the tibial plateaux, and not pulling forward as when the knee was extended. Actually, when the knee extension increases, ligament tension switches from the PCL (that completely relaxes at 20% of the gait cycle) to the ACL that quite suddenly becomes tensioned and remains loaded for the remining stance phase, in which the VM and VL are activated and exert an anteriorly-directed force via the patellar tendon. Moreover, ACL recruitment is coherent with the gastrocnemii activity, which act as an ACL antagonist. Important contributions to the knee-joint stability during the stance phase are provided by all components of the capsula (although with different patterns) and by both the superficial and deep components of the MCL. During the swing phase and early stance, the LCL and MCL appear involved as well, consistently with the relatively high degree of knee flexion. Their tension contributes to sustaining the weight and inertia forces of the leg and foot when they are suspended off

the ground, and to providing stability at the early support phase when the foot is placed on the upper step.

Our model is not without limitations, mainly related to the lack of an interface between articular surfaces of the femur and tibia representing the cartilage and the menisci, and to the difficulty of easily adapting the model to different sizes, mainly due to the delicate procedure of ligaments' repositioning. Hence, at present, it can be considered a generic model and therefore the results of this study cannot be generalized to every subject. However, our musculoskeletal model contains the relevant functional elements and allows for a dynamic simulation of what should happen if specific isolated elements are changed.

5. Conclusions

This study investigated the loads distribution on internal knee-joint structures during stair climbing, pointing out how the ligament tensions were related to the joint kinematics and muscle forces. The adoption of our dynamic musculoskeletal model gave us the possibility of conducting a non-invasive study, although limited, of a single exemplary subject. The main features of the tibiofemoral contact force were in perfect agreement with the data measured in vivo, making us confident about the accuracy of our predictions concerning muscle force and ligament tension. The PCL and the deep fibres of the MCL were the most loaded ligamentous structures. Specifically, the mid-swing phase was critical for these ligaments, due to the large knee flexion and the hamstring force needed to reduce the forward acceleration of the limb. The ACL and the fibrous capsule were mainly recruited during the stance phase, while the LCL and the superficial bundles of the MCL stabilized the knee during the swing phase. The ACL recruitment was coherent with both the activation of the vasti muscles during the knee extension (anteriorly-directed force transmitted to the tibia via the patellar tendon) and the simultaneous activation of gastrocnemii (antagonist of this ligament). In this study, the relationship between the muscle forces and the recruitment of the knee-joint ligaments was deepened and our results could be useful for explaining some eventual compensatory strategies during stair climbing: for example, in case of ACL injury, the reduction of the quadriceps force during the stance phase appears justified by the need to reduce the recruitment of this ligament; the reduction of hamstring activity during the swing phase could be explained, in case of a PCL lesion, as a way to relieve this ligament tension. However, further studies should be specially designed to better understand and test these compensatory mechanisms.

A deeper investigation should also be dedicated to the effects of the relationship between step geometry and the subject's size, since joint kinematics, muscular effort, and consequently, the load on the ligaments, are certainly affected by these parameters.

Although this study refers to the action of an intact knee during a task performed by a physiologic subject, the considerations obtained from the comparison of muscle forces and ligament tensions can be useful in a clinical context to identify possible risk of tissue damage, to provide informed recommendations to subjects with ligament injuries, and to suggest potential compensatory strategies for the reduction of the ligament loads.

Author Contributions: Conceptualization, C.A.F. and L.D.; methodology, C.A.F. and L.D.; software, C.A.F., M.G. and L.D.; investigation and data interpretation, C.A.F. and L.D.; resources, C.A.F.; data curation, C.A.F., M.G. and L.D.; writing—original draft preparation, C.A.F. and L.D.; writing—review and editing, C.A.F., M.G. and L.D.; visualization, C.A.F. and L.D. All authors have read and agreed to the published version of the manuscript.

Funding: This research received no external funding.

Institutional Review Board Statement: Not applicable.

Informed Consent Statement: Not applicable.

Data Availability Statement: The data presented in this study are available on request from the corresponding author.

Acknowledgments: This work is part of a PhD project (Lucia Donno), supported by the Ministry of University and Research, Politecnico di Milano, 37th cycle.

Conflicts of Interest: The authors declare no conflict of interest.

References

1. Boreham, C.A.G.; Wallace, W.F.M.; Nevill, A. Training Effects of Accumulated Daily Stair-Climbing Exercise in Previously Sedentary Young Women. *Prev. Med.* **2000**, *30*, 277–281. [CrossRef]
2. Boreham, C.A.G. Training Effects of Short Bouts of Stair Climbing on Cardiorespiratory Fitness, Blood Lipids, and Homocysteine in Sedentary Young Women. *Br. J. Sports Med.* **2005**, *39*, 590–593. [CrossRef] [PubMed]
3. Handsaker, J.C.; Brown, S.J.; Bowling, F.L.; Maganaris, C.N.; Boulton, A.J.M.; Reeves, N.D. Resistance Exercise Training Increases Lower Limb Speed of Strength Generation during Stair Ascent and Descent in People with Diabetic Peripheral Neuropathy. *Diabet. Med.* **2016**, *33*, 97–104. [CrossRef] [PubMed]
4. Donath, L.; Faude, O.; Roth, R.; Zahner, L. Effects of Stair-Climbing on Balance, Gait, Strength, Resting Heart Rate, and Submaximal Endurance in Healthy Seniors: Stair-Climbing in Healthy Seniors. *Scand. J. Med. Sci. Sports* **2014**, *24*, e93–e101. [CrossRef] [PubMed]
5. Zachazewski, J.E.; Riley, P.O.; Krebs, D.E. Biomechanical Analysis of Body Mass Transfer during Stair Ascent and Descent of Healthy Subjects. *J. Rehabil. Res. Dev.* **1993**, *30*, 412–422.
6. Riener, R.; Rabuffetti, M.; Frigo, C. Stair Ascent and Descent at Different Inclinations. *Gait Posture* **2002**, *15*, 32–44. [CrossRef]
7. Protopapadaki, A.; Drechsler, W.I.; Cramp, M.C.; Coutts, F.J.; Scott, O.M. Hip, Knee, Ankle Kinematics and Kinetics during Stair Ascent and Descent in Healthy Young Individuals. *Clin. Biomech.* **2007**, *22*, 203–210. [CrossRef]
8. Novak, A.C.; Li, Q.; Yang, S.; Brouwer, B. Mechanical Energy Transfers across Lower Limb Segments during Stair Ascent and Descent in Young and Healthy Older Adults. *Gait Posture* **2011**, *34*, 384–390. [CrossRef]
9. Nadeau, S.; McFadyen, B.J.; Malouin, F. Frontal and Sagittal Plane Analyses of the Stair Climbing Task in Healthy Adults Aged over 40 Years: What Are the Challenges Compared to Level Walking? *Clin. Biomech.* **2003**, *18*, 950–959. [CrossRef]
10. Byrapogu, V.K.; Gale, T.; Hamlin, B.; Urish, K.L.; Anderst, W. Medial Unicompartmental Knee Arthroplasty Restores Native Knee Kinematics during Activities of Daily Living: A Pilot Study. *Ann. Biomed. Eng.* **2023**, *51*, 308–317. [CrossRef]
11. Hamai, S.; Okazaki, K.; Shimoto, T.; Nakahara, H.; Higaki, H.; Iwamoto, Y. Continuous Sagittal Radiological Evaluation of Stair-Climbing in Cruciate-Retaining and Posterior-Stabilized Total Knee Arthroplasties Using Image-Matching Techniques. *J. Arthroplast.* **2015**, *30*, 864–869. [CrossRef]
12. Hawker, G.A.; Bohm, E.; Dunbar, M.J.; Faris, P.; Jones, C.A.; Noseworthy, T.; Ravi, B.; Woodhouse, L.J.; Marshall, D.A. Patient Appropriateness for Total Knee Arthroplasty and Predicted Probability of a Good Outcome. *RMD Open* **2023**, *9*, e002808. [CrossRef]
13. Lützner, J.; Beyer, F.; Lützner, C.; Riedel, R.; Tille, E. Ultracongruent Insert Design Is a Safe Alternative to Posterior Cruciate-Substituting Total Knee Arthroplasty: 5-Year Results of a Randomized Controlled Trial. *Knee Surg. Sports Traumatol. Arthrosc.* **2022**, *30*, 3000–3006. [CrossRef]
14. Di Fabio, R.P.; Zampieri, C.; Tuite, P. Gaze Control and Foot Kinematics During Stair Climbing: Characteristics Leading to Fall Risk in Progressive Supranuclear Palsy. *Phys. Ther.* **2008**, *88*, 240–250. [CrossRef] [PubMed]
15. Graci, V.; Rabuffetti, M.; Frigo, C.; Ferrarin, M. Is Lower Peripheral Information Weighted Differently as a Function of Step Number during Step Climbing? *Gait Posture* **2017**, *52*, 52–56. [CrossRef] [PubMed]
16. Lee, H.-J.; Chou, L.-S. Balance Control during Stair Negotiation in Older Adults. *J. Biomech.* **2007**, *40*, 2530–2536. [CrossRef] [PubMed]
17. Reeves, N.D.; Spanjaard, M.; Mohagheghi, A.A.; Baltzopoulos, V.; Maganaris, C.N. The Demands of Stair Descent Relative to Maximum Capacities in Elderly and Young Adults. *J. Electromyogr. Kinesiol.* **2008**, *18*, 218–227. [CrossRef]
18. Asay, J.L.; Mündermann, A.; Andriacchi, T.P. Adaptive Patterns of Movement during Stair Climbing in Patients with Knee Osteoarthritis: Adaptive patterns of movement. *J. Orthop. Res.* **2009**, *27*, 325–329. [CrossRef]
19. Kaufman, K.R.; Hughes, C.; Morrey, B.F.; Morrey, M.; An, K.-N. Gait Characteristics of Patients with Knee Osteoarthritis. *J. Biomech.* **2001**, *34*, 907–915. [CrossRef]
20. Taylor, S.J.G.; Walker, P.S.; Perry, J.S.; Cannon, S.R.; Woledge, R. The Forces in the Distal Femur and the Knee during Walking and Other Activities Measured by Telemetry. *J. Arthroplast.* **1998**, *13*, 428–437. [CrossRef]
21. Shelburne, K.B.; Torry, M.R.; Pandy, M.G. Contributions of Muscles, Ligaments, and the Ground-Reaction Force to Tibiofemoral Joint Loading during Normal Gait. *J. Orthop. Res.* **2006**, *24*, 1983–1990. [CrossRef]
22. Kutzner, I.; Heinlein, B.; Graichen, F.; Bender, A.; Rohlmann, A.; Halder, A.; Beier, A.; Bergmann, G. Loading of the Knee Joint during Activities of Daily Living Measured in vivo in Five Subjects. *J. Biomech.* **2010**, *43*, 2164–2173. [CrossRef]
23. Walter, J.P.; Korkmaz, N.; Fregly, B.J.; Pandy, M.G. Contribution of Tibiofemoral Joint Contact to Net Loads at the Knee in Gait: Contribution of Tibiofemoral joint contact. *J. Orthop. Res.* **2015**, *33*, 1054–1060. [CrossRef] [PubMed]
24. Lenhart, R.L.; Kaiser, J.; Smith, C.R.; Thelen, D.G. Prediction and Validation of Load-Dependent Behavior of the Tibiofemoral and Patellofemoral Joints during Movement. *Ann. Biomed. Eng.* **2015**, *43*, 2675–2685. [CrossRef] [PubMed]

25. Bersini, S.; Sansone, V.; Frigo, C.A. A Dynamic Multibody Model of the Physiological Knee to Predict Internal Loads during Movement in Gravitational Field. *Comput. Methods Biomech. Biomed. Eng.* **2016**, *19*, 571–579. [CrossRef]
26. Taylor, W.R.; Heller, M.O.; Bergmann, G.; Duda, G.N. Tibio-Femoral Loading during Human Gait and Stair Climbing. *J. Orthop. Res.* **2004**, *22*, 625–632. [CrossRef] [PubMed]
27. Beynnon, B.D.; Fleming, B.C. Anterior Cruciate Ligament Strain in-vivo: A Review of Previous Work. *J. Biomech.* **1998**, *31*, 519–525. [CrossRef]
28. Cerulli, G.; Benoit, D.L.; Lamontagne, M.; Caraffa, A.; Liti, A. In vivo Anterior Cruciate Ligament Strain Behaviour during a Rapid Deceleration Movement: Case Report. *Knee Surg. Sports Traumatol. Arthrosc.* **2003**, *11*, 307–311. [CrossRef]
29. Fleming, B.C.; Beynnon, B.D.; Renstrom, P.A.; Johnson, R.J.; Nichols, C.E.; Peura, G.D.; Uh, B.S. The Strain Behavior of the Anterior Cruciate Ligament During Stair Climbing: An in vivo Study. *Arthrosc. J. Arthrosc. Relat. Surg.* **1999**, *15*, 185–191. [CrossRef]
30. Frigo, C.A.; Donno, L. The Effects of External Loads and Muscle Forces on the Knee Joint Ligaments during Walking: A Musculoskeletal Model Study. *Appl. Sci.* **2021**, *11*, 2356. [CrossRef]
31. Grood, E.S.; Suntay, W.J. A Joint Coordinate System for the Clinical Description of Three-Dimensional Motions: Application to the Knee. *J. Biomech. Eng.* **1983**, *105*, 136–144. [CrossRef]
32. Donno, L.; Frigo, C.A. The Effects of Anterior Cruciate Ligament Sacrifice on the Behavior of the Knee Joint, Tested through the Use of a Musculoskeletal Model. *Gait Posture* **2022**, *97*, 1. [CrossRef]
33. Donno, L.; Sansone, V.; Galluzzo, A.; Frigo, C.A. Walking in the Absence of Anterior Cruciate Ligament: The Role of the Quadriceps and Hamstrings. *Appl. Sci.* **2022**, *12*, 8667. [CrossRef]
34. Blankevoort, L.; Huiskes, R.; De Lange, A. Recruitment of Knee Joint Ligaments. *J. Biomech. Eng.* **1991**, *113*, 94–103. [CrossRef]
35. Rasmussen, J.; Damsgaard, M.; Voigt, M. Muscle Recruitment by the Min/Max Criterion—A Comparative Numerical Study. *J. Biomech.* **2001**, *34*, 409–415. [CrossRef]
36. Andriacchi, T.P.; Andersson, G.B.; Fermier, R.W.; Stern, D.; Galante, J.O. A Study of Lower-Limb Mechanics during Stair-Climbing. *J. Bone Jt. Surg. Am.* **1980**, *62*, 749–757. [CrossRef]
37. Gregor, R.J.; Cavanagh, P.R.; LaFortune, M. Knee Flexor Moments during Propulsion in Cycling—A Creative Solution to Lombard's Paradox. *J. Biomech.* **1985**, *18*, 307–316. [CrossRef]
38. Andrews, J.G. The Functional Roles of the Hamstrings and Quadriceps during Cycling: Lombard's Paradox Revisited. *J. Biomech.* **1987**, *20*, 565–575. [CrossRef] [PubMed]
39. Lombard, W.P.; Abbott, F.M. The mechanical effects produced by the contraction of individual muscles of the thigh of the frog. *Am. J. Physiol.-Leg. Content* **1907**, *20*, 1–60. [CrossRef]
40. Frigo, C.; Pavan, E.E.; Brunner, R. A Dynamic Model of Quadriceps and Hamstrings Function. *Gait Posture* **2010**, *31*, 100–103. [CrossRef] [PubMed]